Proceedings of JPGC'01
2001 International Joint Power Generation Conference
New Orleans, Louisiana, June 4–7, 2001

JPGC2001/PWR-19171

CYCLE ANALYSIS OF GAS TURBINE-FUEL CELL HYBRID MICRO GENERATION SYSTEM

Hideyuki Uechi* **Shinji Kimijima** **Nobuhide Kasagi**

The University of Tokyo
Department of Mechanical Engineering
Hongo 7-3-1, Bunkyo-ku, Tokyo 113-8656, Japan

ABSTRACT

Small distributed generation systems are currently attracting much attention because of their high energy utilization efficiency. Among them, a hybrid system based on micro gas turbine (μGT) and solid oxide fuel cell (SOFC) is expected to achieve much higher efficiency than a traditional μGT. In this paper, we investigate the effects of cycle design parameters on the performance and feasibility of a μGT-SOFC hybrid system for small apartments and businesses. As a result, a general design strategy is found that less direct fuel input to combustor as well as higher recuperator effectiveness leads to higher generation efficiency, while higher steam-carbon ratio moderates requirements for the material strength. It is also confirmed that the hybrid system is much superior to the recuperated gas turbine in terms of its power efficiency and aptitude for small distributed generation. A conceptual design of a 30kW μGT-SOFC hybrid system, of which diameter and height are 750mm and 1500mm, respectively, is shown to give power efficiency over 65% (LHV) in the best possible case.

NOMENCLATURE

Symbols

F :	Farady constant	C/mol
G :	Gibbs free energy	J/kg
H :	enthalpy	W
J :	cell current density	A/ m^2
K :	equilibrium constant	
Q :	heat	W
R :	gas constant	J/mol K
T :	temperature	K
V :	voltage	V
W:	power	W
i :	current	A
n :	number of moles	mol
p :	pressure	atm
x :	mole fraction	
δ :	thickness	mm
η :	efficiency	
ρ :	electrical resistance	Ω cm

Subscripts

cell : SOFC cell
ref : reforming or reformer
shf : shifing
an : anode
ca : cathode
el : electrolyte
net : net value
act : activation porarization
SOFC : solid oxide fuel cell
c : compressor
t : turbine
DA : inverter
gen : generater

* Present Address: Mitsubishi Heavy Industries, Ltd., Takasago Research and Development center, 2-1-1, Arai-cho, Shinhama, Takasago-City, Hyogo 676-8686, Japan

gcfc : gas compressor for SOFC

gcgt : gas compressor for combustor

blow : blower

in : inlet

out : outlet

1. INTRODUCTION

Recently, energy saving has become even more important to mitigate possible climate change due to emission of carbon dioxide. Small distributed generation systems, which make it possible to utilize exhaust heat of generation process, are expected to achieve higher efficiency energy utilization. Now, micro gas turbines (μGT) under 100kW are in practical use [1]. Even smaller μGT as 5kW has a perspective to be realized [2]. Moreover, μGTs have possibility to achieve such high efficiency as 40% with higher turbine inlet temperature (TIT) and recuperator effectiveness [2].

It is, however, difficult to achieve much higher efficiency than 40% using traditional μGT, while a μGT combined with a fuel cell (FC), especially a solid oxide fuel cell (SOFC) is expected to attain extremely higher efficiency. It is already shown that the μGT-SOFC hybrid system offers efficiency over 70% [3]. Recently 100kW and 220kW systems are on trial operation [4].

Although past studies were mainly aimed at systems over 100kW, even smaller systems are necessary to meet increasing civilian energy demand, and to popularize the hybrid system. It is probable that popularization can decrease costs of SOFC. In this paper, a 30kW μGT-SOFC hybrid system for small businesses and small apartments is investigated. We show the effectiveness and features of μGT-SOFC hybrid system through an exergy analysis. Cycle calculations are performed to clarify the effects of cycle parameters on the cycle performance and to find design strategy. The conceptual design of a 30 kW μGT-SOFC hybrid system is also made to estimate the size and efficiency of the system in the best possible case.

2. SYSTEM CONFIGURATION

Figure 1 shows the configuration of a μGT-SOFC hybrid system. The numerical specifications in this figure are those obtained in a typical case. The system is fed with methane at atmospheric temperature and pressure as fuel.

In this cycle, air compressed by a compressor and preheated in a recuperator is supplied into the cathode of SOFC. Cathode outlet air is utilized to burn residual hydrogen, carbon oxide, and methane in anode outlet gas with additional methane injected into a combustor. The combustor outlet gas drives a turbine and heats compressor outlet gas in the recuperator. The reformer is supplied with a mixture of methane and anode outlet gases. Methane is reformed by using steam from the anode outlet as well as heat from the cell.

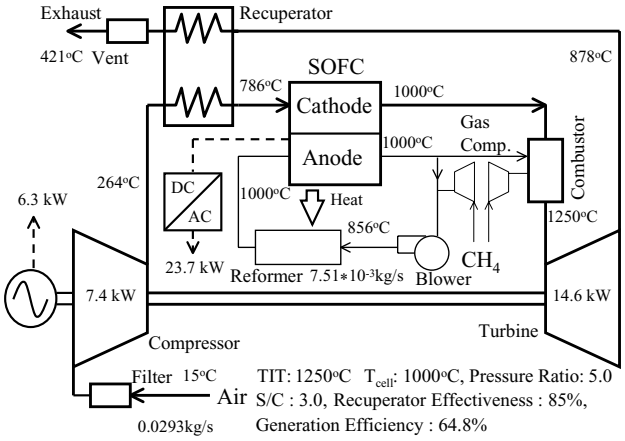

Fig. 1 μGT-SOFC hybrid system

Table. 1 Cycle analysis conditions

Cell Temperature (°C)	1000
Turbine Inlet Temperature (°C)	Variable
Pressure Ratio (-)	5.0
Total Electric Power Output (kW)	30
Recuperator Effectiveness (%)	85
Compressor Adiabatic Efficiency (%)	73
Turbine Adiabatic Efficiency (%)	80
GT Mechanical Efficiency (%)	95
Blower Adiabatic Efficiency (%)	70
Blower Mechanical Efficiency (%)	90
Gas Compressor Adiabatic Efficiency (%)	60
Gas Compressor Mechanical Efficiency (%)	90
Steam Carbon Ratio (-)	3
Current Density (A/m^2)	3000
H_2 Utilization Ratio (%)	80
Cathode Thickness (mm)	2
Anode Thickness (mm)	0.1
Electrolyte Thickness (mm)	0.02
SOFC Pressure Drop (%)	5
Reformer Pressure Drop (%)	4
Filter Pressure Drop (%)	0.5
Vent Pressure Drop (%)	0.5
Recuperator Pressure Drop (Air Side) (%)	3
Recuperator Pressure Drop (Exhaust Side) (%)	2
Atmospheric Temperature (°C)	15
Generator Efficiency (%)	98
Inverter Efficiency (%)	93

3. CYCLE ANALYSIS

3.1 Assumptions

The basic conditions of the present cycle analysis are shown in Table 1. Unless otherwise stated, these conditions are assumed. We make the following assumptions:

(1) Gases do not leak outside the system.

(2) Heat loss is negligibly small.

(3) Chemical reactions proceed to equilibrium states.

(4) Internal distributions of the temperature, gas composition, and pressure in each system component are not considered.

(5) Steady state operation is considered.

(6) Heat required in the reformer is supplied from the cell.

(7) The anode outlet temperature, the cathode outlet temperature, and the reformer outlet temperature are all equal to the cell temperature.

(8) In the combustor, the residual gas from the anode and the injected methane are burnt completely.

3.2 Reaction Heats and Equilibrium Constants

For analyzing the reaction in the reformer and the cell, the reaction heats and the equilibrium constants should be known. The reaction heats are obtained from the data of the formation enthalpy in JANAF table [5], except the formation enthalpy of methane, of which coefficient is given in the literature [6]. The equilibrium constants are obtained from difference of the Gibbs energies using the following equation:

$$K = Exp\left(-\frac{\Delta G}{RT}\right) \tag{1}$$

The reaction heats and equilibrium constants are expressed as polynomials fitting functions of temperature.

3.3 Micro Gas Turbine

For the calculation of compression and expansion processes in the compressor and turbine, the standard method in the literature [7] is used. The combustor outlet temperature is first assumed, then the combustor methane input is determined by iterative calculation. The power output from the gas turbine is obtained by using the following equation:

$$W_{gt} = \eta_{gen}\left(\eta_{mgt} W_t - W_c\right) - W_{gcgt} \tag{2}$$

3.4 Reformer

In the reformer, hydrogen and carbon oxide are produced from methane and steam. Inside the reformer, the reactions bellow are considered.

reforming: $\mathrm{CH_4 + H_2O \rightarrow 3H_2 + CO}$ (3)

shifting: $\mathrm{CO + H_2O \rightarrow H_2 + CO_2}$ (4)

Reforming is an endothermic reaction, where shifting is an exothermic reaction. As a whole, the reaction in the reformer is endothermic. To allow methane and steam to react, the residual heat in the cell is transferred to the reformer.

The equilibrium constant of reforming K_{ref} and that of shifting K_{shf} are defined based on the partial pressures of species as:

$$K_{ref} = \frac{p_{\mathrm{H_2}}{}^3\, p_{\mathrm{CO}}}{p_{\mathrm{CH_4}}\, p_{\mathrm{H_2O}}} \tag{5}$$

$$K_{shf} = \frac{p_{\mathrm{H_2}}\, p_{\mathrm{CO_2}}}{p_{\mathrm{CO}}\, p_{\mathrm{H_2O}}} \tag{6}$$

We can obtain mole numbers for reforming Δn_{ref}, and for shifting Δn_{shf} by iterative calculation from K_{ref} and K_{shf} obtained using the method in 3.2. To estimate K_{ref} and K_{shf}, we assume that the reformer exit temperature equals the cell temperature, and the reforming temperature equals the arithmetic mean of inlet and outlet temperatures. Once the mole numbers to react are estimated, the reaction heat Q_{ref} can be attained from overall heat balance.

3.5 Fuel Cell

3.5.1 Theoretical voltage

In the cell, hydrogen and carbon oxide reacts and the electric power is generated through the following process:

hydrogen: $\mathrm{H_2 + 1/2O_2 \rightarrow H_2O}$ (7)

carbon oxide: $\mathrm{CO + 1/2\,O_2 \rightarrow CO_2}$ (8)

with ΔG_{H2} representing the change of Gibbs energy before and after the reaction of hydrogen, the theoretical voltage is obtained as follows [8]:

$$V_{\mathrm{H_2}} = -\frac{1}{2F}\Delta G_{\mathrm{H_2}} - \frac{RT}{2F}\ln\left(\frac{p_{an,\mathrm{H_2O}}}{p_{an,\mathrm{H_2}}\sqrt{p_{ca,\mathrm{O_2}}}}\right) \tag{9}$$

Using equation (1), we can obtain:

$$V_{\mathrm{H_2}} = \frac{RT}{2F}\left\{\ln K_{\mathrm{H_2}} - \ln\left(\frac{x_{an,\mathrm{H_2O}}}{x_{an,\mathrm{H_2}}}\right) + \frac{1}{2}\ln\left(x_{ca,\mathrm{O_2}}\, p_{ca}\right)\right\} \tag{10}$$

Similarly, for carbon oxide:

$$V_{\mathrm{CO}} = \frac{RT}{2F}\left\{\ln K_{\mathrm{CO}} - \ln\left(\frac{x_{an,\mathrm{CO_2}}}{x_{an,\mathrm{CO}}}\right) + \frac{1}{2}\ln\left(x_{ca,\mathrm{O_2}}\, p_{ca}\right)\right\} \tag{11}$$

The equilibrium constants are obtained as described in 3.2.

3.5.2 Reacting species

From the definition of equilibrium constants, we can obtain the oxygen partial pressure in the anode as follows:

$$p_{an,\mathrm{O_2}} = \left(\frac{1}{K_{\mathrm{H_2}}}\frac{p_{an,\mathrm{H_2O}}}{p_{an,\mathrm{H_2}}}\right)^2 = \left(\frac{1}{K_{\mathrm{CO}}}\frac{p_{an,\mathrm{CO_2}}}{p_{an,\mathrm{CO}}}\right)^2 \tag{12}$$

Using equation (12), we can confirm that the theoretical voltage of hydrogen (equation (10)) and that of carbon oxide (equation (11)) are equal.

At first, the amount of hydrogen to react is calculated. Then,

we can obtain the amount of carbon oxide to react using equation (12). Using the arithmetic mean of mole numbers at the cell inlet and outlet, the relationship between the amounts of reacting hydrogen and carbon oxide is obtained as:

$$\frac{1}{K_{\mathrm{CO}}}\frac{n_{an,\mathrm{CO}_2}+1/2\Delta n_{\mathrm{co}}}{n_{an,\mathrm{CO}}-1/2\Delta n_{\mathrm{co}}}=\frac{1}{K_{\mathrm{H}_2}}\frac{n_{an,\mathrm{H}_2\mathrm{O}}+1/2\Delta n_{\mathrm{H}_2}}{n_{an,\mathrm{H}_2}-1/2\Delta n_{\mathrm{H}_2}} \quad (13)$$

where Δn_{H2} and Δn_{CO} represent the amounts of reacting hydrogen and carbon oxide, respectively. Introducing Δn_{H2} to equation (13), Δn_{CO} is estimated.

3.5.3 Polarization

In a real cell, the net voltage is lower than the theoretical voltage because of some drops in voltage (polarization). There are three kinds of polarizations, namely, activation polarization, ohmic polarization, and concentration polarization.

The activation polarization is estimated as follows [8]:

$$V_{act}=\left\{V_a\frac{\ln(J_c/J_o)}{\ln(1+J_c/J_o)}\right\}\ln(1+J/J_o) \quad (14)$$

where

$$V_a=0.074\,(T/1273) \quad (15)$$

$$J_o=10^{(-A/T+B)} \quad (16)$$

$$J_c=0.4 \quad (17)$$

The ohmic polarization is estimated as follows [3]:

$$\rho_{an}=0.00298\ Exp\,(-1392/T) \quad (18)$$

$$\rho_{ca}=0.008114\ Exp\,(600/T) \quad (19)$$

$$\rho_{el}=0.00294\ Exp\,(10350/T) \quad (20)$$

The concentration polarization is negligibly small if compared to the other polarizations [8].

3.5.4 SOFC output

Considering the activation and ohmic polarizations, the net voltage of the cell is calculated as:

$$V_{net}=V_{H_2}-V_{act}-J(\rho_{an}\delta_{an}+\rho_{ca}\delta_{ca}+\rho_{el}\delta_{el}) \quad (21)$$

The current is obtained from the amount of reaction species as:

$$i=2F\Delta n_{\mathrm{H}_2}+2F\Delta n_{\mathrm{CO}} \quad (22)$$

Therefore, the SOFC output is:

$$W'_{SOFC}=V_{net}\,i \quad (23)$$

Now, we should take into account the power for SOFC auxiliaries. Then, the SOFC net output is obtained as follows:

$$W_{SOFC}=\eta_{DA}W'_{SOFC}-W_{gcfc}-W_{blow} \quad (24)$$

3.5.5 Cell energy balance

From the total inlet enthalpy H_{in} and the reaction enthalpy ΔH_{cell}, the total cell exit enthalpy H_{out} is obtained as:

$$H_{out}=\{H_{in}+(-\Delta H_{cell})\}-(W'_{SOFC}+Q_{ref}) \quad (25)$$

Assuming that the anode and cathode outlet temperatures are equal, they are obtained from H_{out}. We can derive the fuel input to SOFC for a certain cell temperature by iterative calculation.

A part of the anode exit gas is recirculated. The amount of recirculated gas is obtained from the specified S/C ratio. In this study, the generation efficiency is defined based upon the sum of SOFC and gas turbine heat inputs, which are estimated in terms of the lower heating value.

4. CHARACTERISTICS OF HYBRID SYSTEM

The μGT-SOFC hybrid system is expected to achieve efficiency near 70%. To clarify the major reasons, we performed an exergy analysis (Fig. 2). TIT is increased to 1200°C using a ceramic turbine. Each exergy fraction is defined as the ratio of output or exergy loss to exergy of fuel input. Thus, the exergy fraction of output is not equal to the generation efficiency. The combustion loss of the hybrid is lower than that of traditional recuperated gas turbine, because electric power and heat are generated simultaneously. The exhaust loss and the recuperator loss are lower than that of atmospheric SOFC. With the turbine, additional power is recovered effectively from high temperature exhaust gas. Smaller difference between the high and low temperatures in the recuperator makes the irreversibility of heat transfer decrease.

Generally, smaller power output tends to decrease the generation efficiency. To estimate the effect of reduction in power level on generation efficiency, we performed a cycle analysis for 30kW and 300kW systems of both hybrid system and traditional recuperated gas turbine. We assume that the compressor, turbine and mechanical efficiencies depend on the output level. To give these elemental efficiencies, it is also assumed that approximately one fifth of the total output is gained by the gas turbine. The result is shown in table 2. For the hybrid system, the difference in the heat input per 1kW output between 30kW and 300kW systems is 0.07kW, where that of traditional recuperated gas turbine is 0.23kW. It is evident that the hybrid system efficiency is less dependent on the power output level, so that the hybrid system is more suitable for small systems.

The gas turbines generation efficiency is generally decreased when the intake air temperature is elevated. This tendency is a disadvantage for a small generation system because the demand for electricity is high in summer. We estimated the effect of atmosphere temperature on the generation efficiency. The cycle calculations for compressor inlet temperature of 15°C and 30°C were performed for both a hybrid system and a traditional gas turbine (Table 3). For the hybrid system, the difference of heat input per 1kW output at 15°C and 30°C equals 0.03kW, while that of the traditional recuperated gas turbine is 0.12kW. Thus the hybrid system deteriorates less in its efficiency in summer.

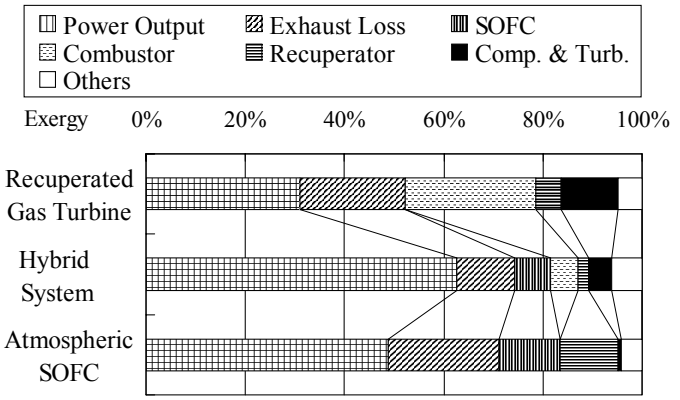

Fig. 2 Breakdown of exergy consumption

Table. 2 Effect of power output capacity

	Recuperated GT		Hybrid System	
Total Output (kW)	30	300	30	300
Pressure Ratio (-)	5.0	6.0	5.0	
Compressor Adiabatic Efficiency (%)	75	79	73	76
Turbine Adiabatic Efficiency (%)	85	87	80	86
GT Mechanical Efficiency (%)	97	98	95	97
Turbine Inlet Temperature (°C)	1250			
Fuel Consumption per 1kW Output (kW)	2.65	2.42	1.54	1.47

Table. 3 Effect of intake air temperature

	Recuperated GT		Hybrid System	
Total Output (kW)	30			
Compressor Inlet Temperature (°C)	15	30	15	30
Pressure Ratio (-)	5.0		5.0	
Compressor Adiabatic Efficiency (%)	75		73	
Turbine Adiabatic Efficiency (%)	85		80	
GT Mechanical Efficiency (%)	97		95	
Turbine Inlet Temperature (°C)	1250			
Fuel Consumption per 1kW Output (kW)	2.65	2.77	1.54	1.57

5. STRATEGY FOR HYBRID SYSTEM DESIGN

Some of the design parameters of a hybrid system are flexible, while the others cannot be changed widely. For example, once the output power is set, the compressor and turbine efficiencies are given, whereas we can choose the pressure ratio rather freely. Here, the effects of cell temperature and of TIT on the cycle performance are shown. Moreover, general strategy to set cycle parameters, such as recuperator temperature effectiveness, S/C ratio, pressure ratio and TIT, is also shown below.

5.1 Effects of Cell Temperature and TIT

While we study the effects of cell temperature and TIT, the other variables are fixed. The generation efficiency is shown in Fig. 3. First, it is clear that higher cell temperature gives higher efficiency. However, unlike a conventional gas turbine, the hybrid system's efficiency is decreased with increasing TIT at a fixed cell temperature. We should remember that higher cell temperature implies higher cost and requires longer time to start up. Therefore, we fix the cell temperature at 1000°C, that is the limit for the state-of-the-art SOFC technology, in the following discussions.

Figure 4 shows the total heat input (thicker line) and the SOFC heat input (thinner line). As a result, the heat input to the

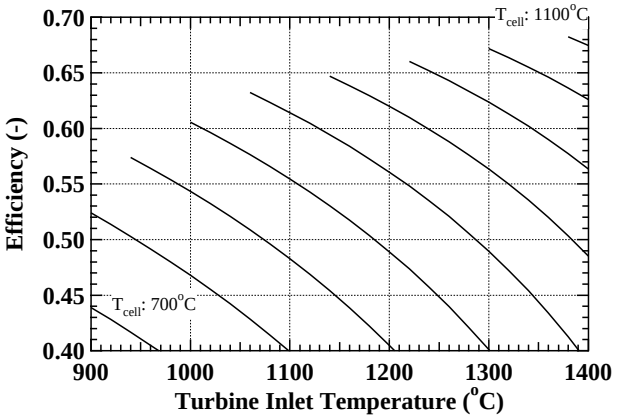

Fig. 3 Power generation efficiency (LHV)

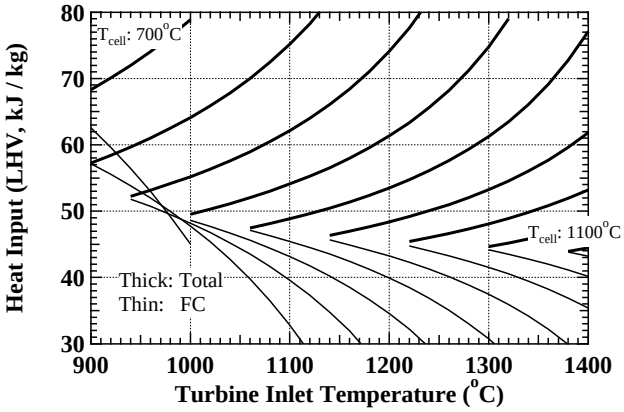

Fig. 4 Heat input

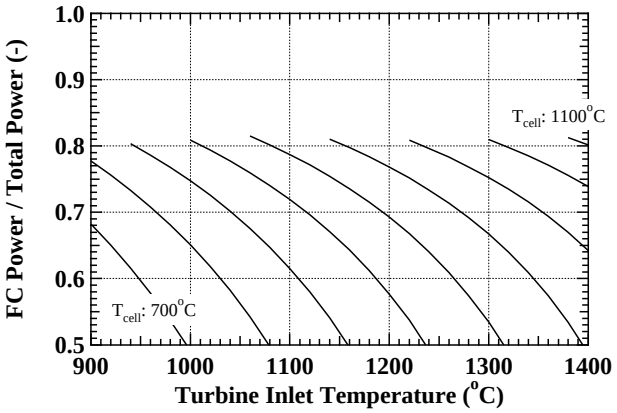

Fig. 5 Fraction of SOFC output

combustor is given as a difference between them. Large direct heat input to the combustor causes high TIT. Thus, it is found that large direct heat input to the combustor reduces total generation efficiency, because the heat input to SOFC is utilized more effectively than is the combustor. This is supported by Fig. 3, in which high TIT or large heat input to the combustor gives low generation efficiency.

It is also evident that there is a certain TIT for each cell temperature with zero heat input to the combustor. We can not lower TIT beyond the temperature that is equivalent to zero heat input.

The ratio of SOFC output to total output is shown in Fig. 5. Higher cell temperature gives higher SOFC fraction, while higher TIT gives lower SOFC fraction. At the lowest TIT for each cell temperature, SOFC fraction is approximately 80%.

5.2 Recuperator Effectiveness

We estimate the effect of recuperator temperature effectiveness on the cycle performance. High recuperator effectiveness leads to high cathode inlet temperature. Thus, the fuel input to SOFC for a unit amount of air is reduced if the cell temperature is fixed. This is confirmed by the decrease in oxygen utilization in SOFC (Fig. 6). Small fuel input to SOFC causes residual gas such as methane, hydrogen and carbon oxide decrease (Fig. 7). Less residual gases lower TIT. Therefore, higher recuperator effectiveness causes lower TIT for a fixed heat input to the combustor (Fig. 8). The generation efficiency (Fig. 9) is increased if the recuperator effectiveness is increased, when TIT is decreased or the fuel input to the combustor is fixed.

5.3 Steam Carbon (S/C) Ratio

S/C ratio is defined as the ratio of the mole fractions of steam and methane at the reformer inlet. The S/C ratio determines the amount of anode recirculation.

When we increase the S/C ratio with other parameters fixed, the amount of anode recirculation or that of anode inlet gas is increased. This results in the reduction of the fuel input to the SOFC at a fixed SOFC outlet temperature. In the same manner, as the recuperator effectiveness is increased, a high S/C ratio causes low TIT where the fuel input to the combustor is fixed (Fig. 10). Figure 11 shows the generation efficiency. Increase in S/C ratio reduces the generation efficiency with fixed TIT. But, if S/C ratio decreases with fixed fuel input to the combustor, reduction of the generation efficiency is not remarkable.

We can decrease the turbine exit temperature with higher S/C ratio and lower TIT. If S/C ratio is increased, for example, from 3.0 to 4.0, minimal TIT decreases from 1210°C to 1165°C. Simul-

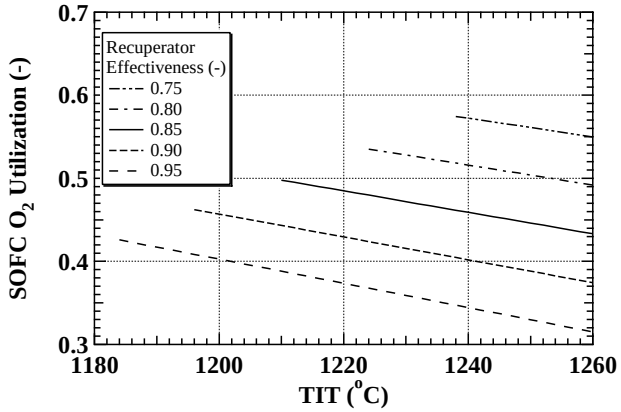

Fig. 6 O_2 utilization in SOFC

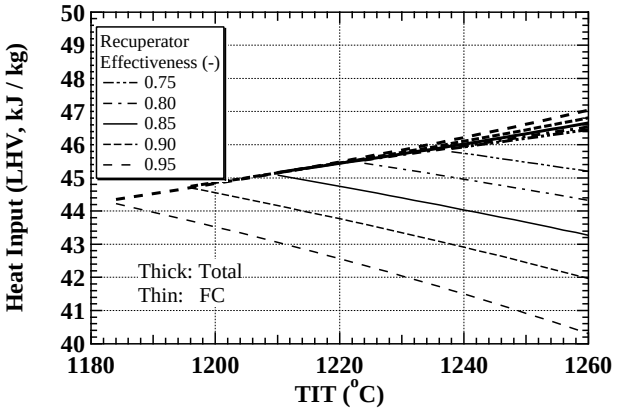

Fig. 8 Heat input

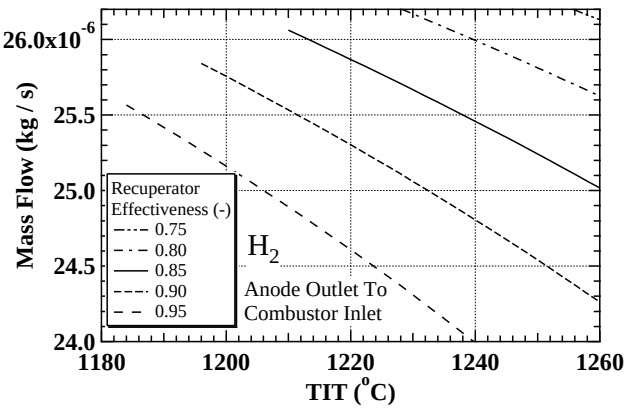

Fig. 7 H_2 mass flow into combustor

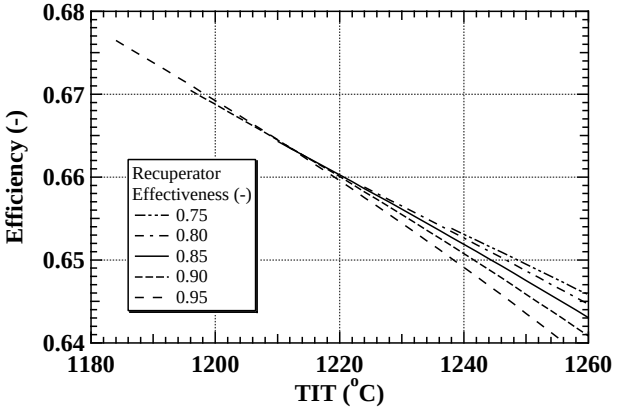

Fig. 9 Power generation efficiency (LHV)

taneously, the turbine exit temperature is lowered from 845°C to 810°C. There is a maximum temperature for the use of metallic recuperators between 850°C and 900°C. Beyond this temperature, we should utilize ceramic recuperators with much more cost [2]. High S/C ratio may enable us to adopt metallic recuperators, and this is favorable even if some reduction of the generation efficiency is considered.

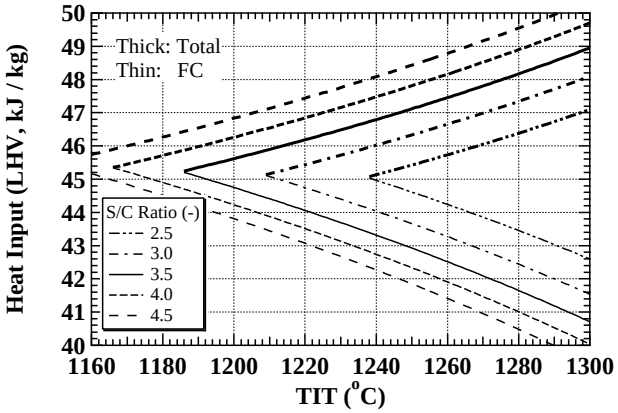

Fig. 10 Heat input

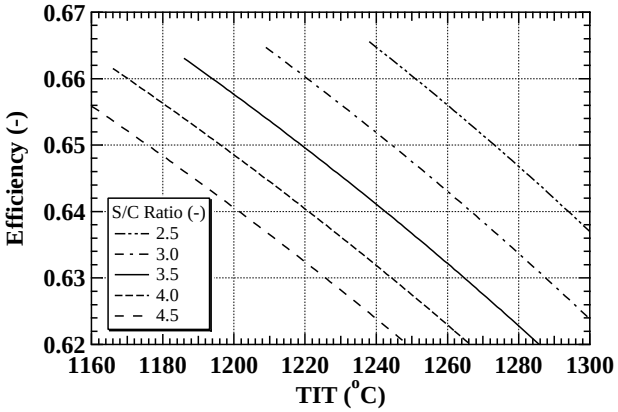

Fig. 11 Power generation efficiency (LHV)

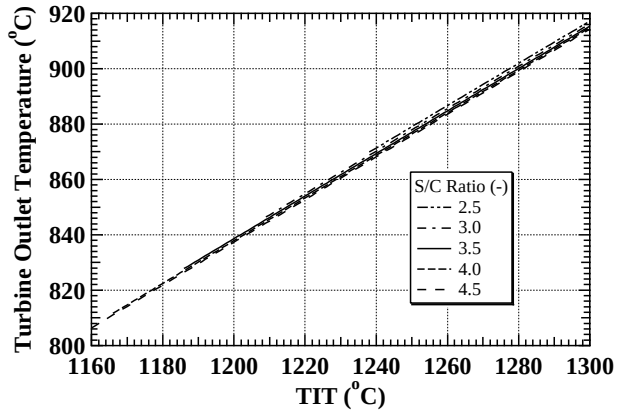

Fig. 12 Turbine outlet temperature

5.4 Pressure Ratio

So far, it is clarified that high recuperator effectiveness is preferable as well as a high S/C ratio moderates the requirement of the temperature increase. We set recuperator effectiveness at 95% [2], and S/C ratio at 4.0 in the following discussions.

To optimize the system pressure and TIT, we performed cycle calculation. Figure 13 shows the effect of pressure ratio on generation efficiency. The maximum efficiency is approximately 67% (LHV) at pressure ratio 4.5 with zero direct heat input to the combustor. However, variation of the maximum generation efficiency from pressure ratio 2.5 to 6.0 is not remarkable.

Higher pressure ratio reduces the turbine outlet temperature and cathode inlet temperature. Low cathode inlet temperature causes high SOFC fuel input. Contrary to the effects of recuperator effectiveness and S/C ratio, higher pressure ratio gives higher TIT. Thus, it is clear that TIT depends on the pressure ratio. We plot heat input in Fig. 14 to determine TIT. Smaller direct fuel input to the combustor is preferable, but a certain amount of fuel input is necessary to burn anode residual gases completely. Assuming that the heat input to the combustor is 1.5kW, we can estimate TIT =1150°C in Fig. 14 for a pressure ratio of 4.0. At this point, the ideal cell voltage is 0.863V, and the net cell voltage is 0.704V. This difference of 0.159V is due to polarization (Fig. 15).

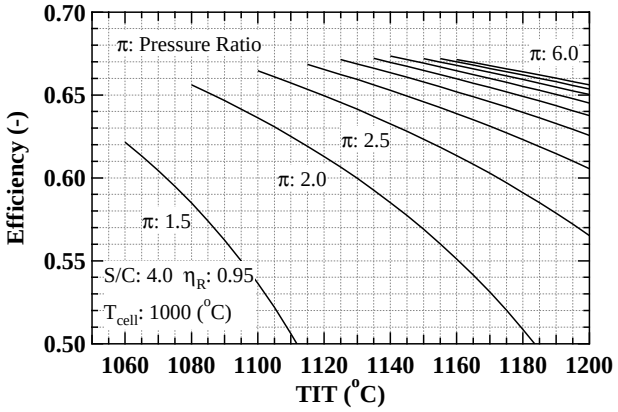

Fig. 13 Power generation efficiency (LHV)

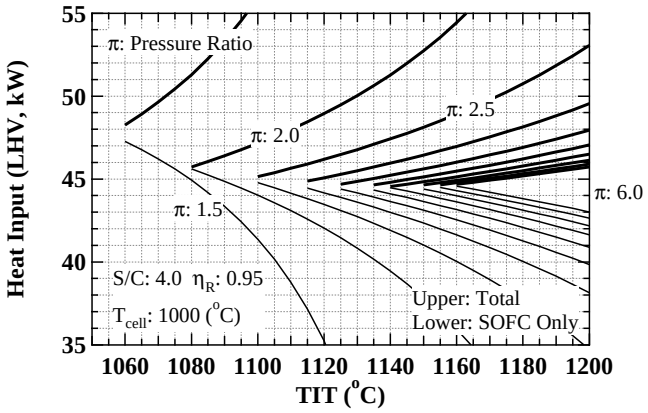

Fig. 14 Heat input

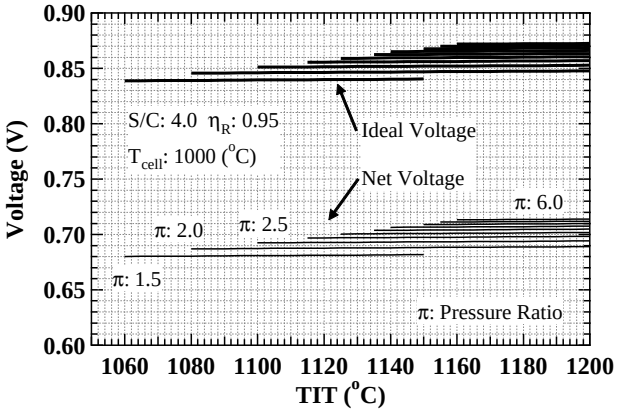

Fig. 15 Cell Voltage

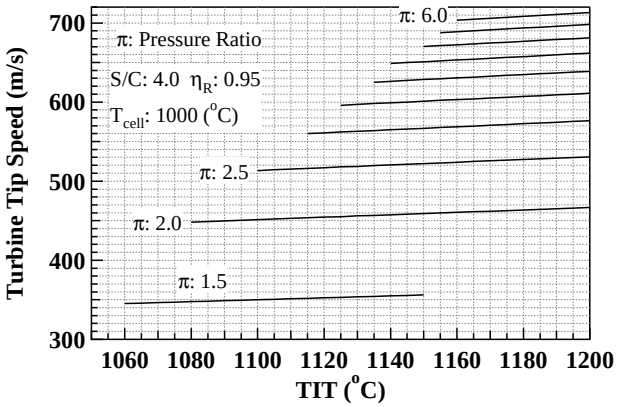

Fig. 16 Estimated turbine tip speed

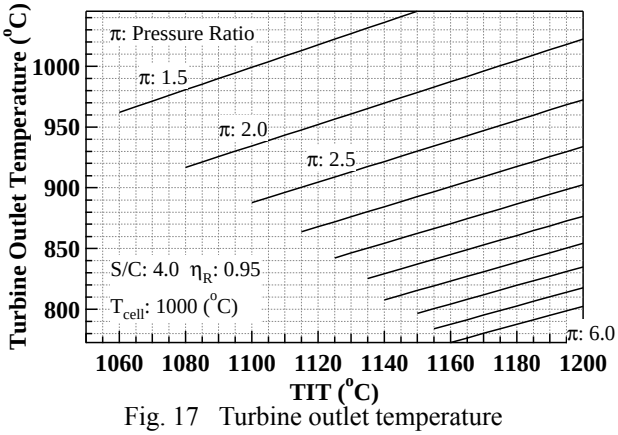

Fig. 17 Turbine outlet temperature

We should also account for the aspects of strength and high-temperature durability of materials. Lower turbine tip speed, which causes lower turbine stress, is desirable. Low turbine outlet temperature is also preferred because it enables us to utilize inexpensive materials for recuperators. The turbine tip speed (Fig. 16) increases as the pressure ratio increases contrary to turbine outlet temperature (Fig. 17). Therefore, we should compromise them. For pressure ratio 4.0 and TIT 1150°C, the turbine tip speed is approximately 630m/s and the turbine outlet temperature is 840°C. These values should be technologically feasible in the foreseeable future.

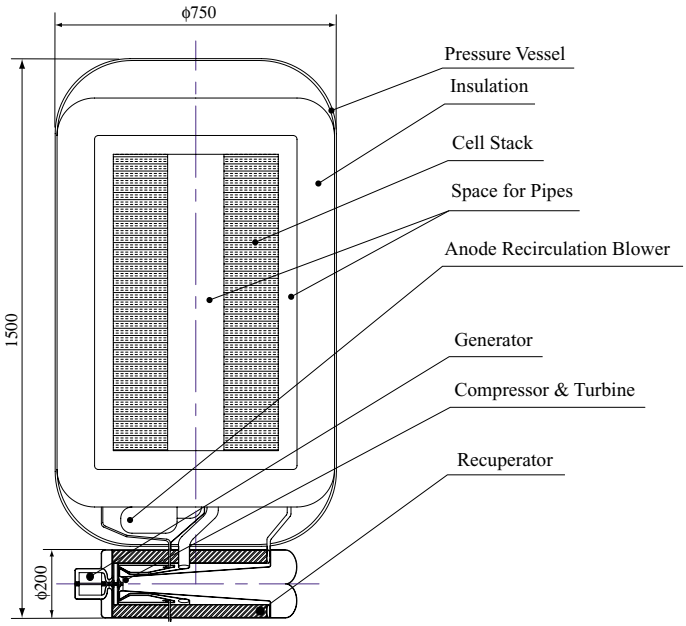

Fig. 18 Conceptual design

6. CONCEPTUAL DESIGN

We performed a conceptual design of a 30kW μGT-SOFC hybrid system for the best possible case. As mentioned above, we set pressure ratio at 4.0, TIT at 1150°C, S/C ratio at 4.0, and recuperator effectiveness as 0.95. The total area of the cell is estimated from the cell current required divided by the current density. The thickness of the cell is estimated from an existing research model of SOFC [9], whose thickness is 5mm. We consider 3mm for reformer and supports. Then, the thickness of a single cell is 8mm. The conceptual design is shown in Fig. 18. The overall size is about of a refrigerator for home use.

7. CONCLUSIONS

Cycle calculations of μGT-SOFC hybrid systems and a conceptual design of a hybrid system for the best possible case are carried out. The following conclusions are derived:

(1) μGT-SOFC hybrid system has potential to achieve high efficiency as high as 65% (LHV), even for a small system of 30kW.

(2) Hybrid systems have higher generation efficiency than that of traditional recuperated gas turbines or atmospheric SOFC, because the exergy loss of combustion and exhaust is much lower.

(3) Output capacity and ambient temperature have smaller influence on the hybrid system than on traditional recuperated gas turbine systems.

(4) Lower amount of direct fuel input to the combustor increases generation efficiency.

(5) Amount of direct fuel input to the combustor depends not only on TIT, but also on other parameters such as recuperator effectiveness, S/C ratio and pressure ratio.

(6) Higher recuperator efficiency gives higher generation efficiency and lower TIT.

(7) Higher S/C ratio lowers TIT and turbine outlet temperature, although it causes a little decrease in generation efficiency.

(8) A certain pressure ratio gives the maximum generation efficiency, but variation of generation efficiency near the optimal pressure ratio is not remarkable.

(9) The diameter of 30kW μGT-SOFC hybrid system is estimated as about 750mm, and its height 1500mm.

ACKNOWLEDGMENTS

This work was supported through the research project on "Micro Gas Turbine/Solid Oxide Fuel Cell Hybrid Cycles for Distributed Energy System" by the Department of Core Research for Evolutional Science and Technology (CREST) of the Ministry of Education, Culture, Sports, Science and Technology (MEXT).

REFERENCES

(1) Craig, P. (1997) "The Capstone Turbogenerator as an Alternative Power Source", SAE Paper, 970292.

(2) McDonald, C. F. (2000) "Low Cost Recuperator Concept for Microturbine Applications", ASME paper, 2000-GT-167.

(3) Massardo, A. F. & Lubelli, F. (2000) "Internal Reforming Solid Oxide Fuel Cell-Gas Turbine Combined Cycles (IRSOFC-GT) : Part A - Cell Model and Cycle Thermodynamic Analysis", Trans. ASME J. of Engineering for Gas Turbine and Power, 122, 27-35.

(4) George, A. R. (2000) "Status of tubular SOFC field unit demonstrations", J. of Power Sources, 86, pp. 134-139.

(5) Malcolm, W. (1989) "NIST-JANAF Thermochemical Tables Fourth Edition", Part1-Part2, American Chemical Society & American Institute of Physics.

(6) Hougen, O. A., Watson, K. M. & Ragatz, R. A. (1959) "Chemical process principles. part II, Thermodynamics", Appendix, John Wiley & Sons, Inc., New York.

(7) Matsunaga, N., Hoshino, T. & Nagashima, A. (1983) "Critical Assessment of Thermophysical Properties Data of Combustion Gases for Calculating the Performance of Gas Turbine", IGTC Paper, 83-TOKYO-IGTC-41.

(8) Nagata, S., Onda, K., Momma, A., Kasuga, Y. & Kato, K. (1993) "Simulation of Temperature Dependence of SOFC and SOE", Bulletine of the Electrotechnical Laboratory, 57-5, 6, pp. 598-615 (in Japanese).

(9) Sakaki, Y., Hattori, M., Nakanishi, A., Aiki, H., Takenobu, K. & Miyamoto, H. (2000) "Development of MOLB Type SOFC", Proc. of The 7th National Symposium on Power and Energy Systems (SPES 2000), JSME, pp. 150-153 (in Japanese).